DLSU Research Congress 2025
De La Salle University, Manila, Philippines
June 26 to 28, 2025

Graphene Oxide/Indium Tin Oxide based Triboelectric nanogenetor (GiTO-TENG) for self-powering small-scale devices.

Mitzi Ramiah S. Garcia[1], Jose M. Esmeria Jr. [2*] and Virgilio D. Ebajo, Jr.[1]
[1] Department of Chemistry, De La Salle University, 2401 Taft Ave., Manila 1004, Philippines
[2] Central Instrumentation Facility, De La Salle University- Laguna Campus, LTAI-Spine Rd, Brgy., Biñan & Malamig City of Biñan, Laguna 4024, Philippines
**Corresponding Author: jose.esmeria@dlsu.edu.ph*

Abstract: Affordable and clean energy is one of the key goals of sustainable development. Generating electrical power through materials that harness electrostatic charges through triboelectricity is a promising source of clean energy. Triboelectric nanogenetor (TENGs) are small, self-powering devices that harvest ambient mechanical energy to generate electricity through triboelectrification. Triboelectrification is a phenomenon wherein two materials of opposite electron affinity contact and separate, generating electrostatic charges of opposite polarity on the surfaces of each material. Electric field induction via a metallic electrode can harness these charges as current, creating a potential difference in powering up a device. In this study, we fabricated a compact TENG using a Vertical contact separation (VCS) design with two materials of opposite charge affinity. The TENG uses a single layer of Graphene Oxide (GO) film as the lower negatively charged material and an Indium Tin Oxide (ITO) film as the upper positively charged layer. The GiTO-TENG generated a peak-to-peak open circuit voltage of 348 Volts. With an active area of 400mm2, this device generated a maximum power density of 30.34mW/m^2 and a current of 0.78μA across a load resistor of 20MΩ.

Key Words: TENG; energy harvesting; Graphene; ITO

1. INTRODUCTION

1.1 Triboelectrification and TENG

Renewable power sources, such as wind, are becoming widely accepted in generating electricity, and solar has been primarily applied to supply energy from small communities to large cities. The " macro" source of renewable energy supports circular economies and sustainable energy goals(Lin et al., 2016). However, small wearable electronics and devices that draw" nano" energy still require batteries for operations. Piezoelectric materials are promising sources of self-power devices, but these materials have less power density (Macá et al., 2022). Triboelectric nanogenerators (TENGs) are promising devices that can produce electricity using widely available common materials and harvest day-to-day mechanical movement.

Triboelectric nanogenerators, or TENGs, are small scale devices that harvest ambient mechanical energy generate electricity through triboelectricity. Triboelectricity is the phenomenon were two

materials contact and separate either by lateral friction or perpendicular force application. When the two materials separate, charges of opposite polarity are generated. Ideally, the materials should be located at both ends of the triboelectric series (Olson & Marks, 2024); one is an electron donor (positively charged), and the other is an electron acceptor (negatively charged). However, reports show that even the same material can generate triboelectrification(Sobarzo Ponce, 2023)

The phenomena of triboelectrification are well known, but the exact theory behind its process is not fully established. Recently, triboelectricity has been proposed to be the overlapping of the electron clouds of contacting materials (Wang & Wang, 2019), which results in the transfer of electron charges from one surface to the other. Also, it was proposed that triboelectrification happens due to the exchange of ionic species(Fang et al., 2024). The high surface charge density generated during triboelectrification produces very high electrostatic potential when separating two materials. By taking advantage of this phenomenon, the TENG was developed by Z.L. Wang et. in 2012 (Wang, 2013). Since then, numerous TENG configurations and investigated materials that consisted of solid waste, natural polymers, cellulose, and complexed synthesized materials were proposed for applications ranging from small health sensors to mini power stations(Lin et al., 2016) . One of the promising materials for TENG applications is graphene. Due to its good electrical conductivity, graphene has been chosen for TENG electrodes and charge storage material. Numerous works on graphene-based TENGs have proposed applications for tactile, humidity, and wearable applications. It is typical that most graphene-based TENG involves additional layers to generate a sufficient amount of electrical output (Chakraborthy et al., 2024) since graphene and graphene oxide are located in the lower middle (negative) of the triboelectric series (Seol et al., 2018). The ITO film, on the other hand, lies on the upper portion of the triboelectric series (positive) because of its metal oxide nature(Zhang & Olin, 2020), (Navaneeth et al., 2023)ITO films are commercially available, and commonly deposited in either glass or PET substrate. In this study, we fabricated a TENG, in which the graphene oxide (1XGO) is directly the negative tribo-layer while the ITO film acts as the opposite positive layer. A TENG device with a graphene oxide having higher oxidation (3XGO) serving as the negative layer was also tested. Both devices have a compact dimension of 20mm x 20mm and generated a significantly higher open circuit voltage than previously published work using similar materials (Shankaregowda et al., 2016).

1.2 Vertical Contact-Separation TENG.

There are two popular modes of TENG operation: vertical contact separation (VCS) and lateral sliding (LS) movement(Wang, 2013). This study used VCS mode since it is less prone to wear and tear. VCS Teng is composed of upper and lower assembly with materials of dielectric constant ε_1 and ε_2, respectively, shown in Figure 1.

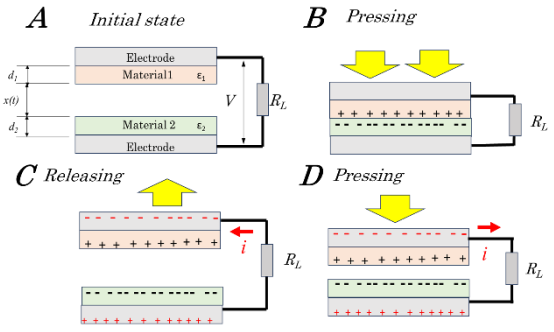

Fig. 1, The process of Vertical Contact-Separation or VCS . The maximum output voltage is attained at *C* when the ideal x(t) separation distance is achieved.

When a downward force is applied from its initial state in *A*, two surfaces contact in step *B*, and when the force is released and two materials separate in *C*, opposite charges are generated on each surface, and the maximum voltage is attained when the *x(t)* is

maximum. At this point, the charges on electrodes are induced from the materials, and the flows are current. When the upper assembly is pressed again, the distance *x(t)* is reduced, such that the potential difference *V*, is also reduced.

1.3 V-Q-x relationship in VCS TENG

VCS TENG follows the *V-Q-x* principle, wherein the output voltage, *V*, is directly related to the amount of charge transferred, *Q*, and the separation distance *x* between the two materials. This process can be explained in Equation 1 (H. Chen et al., 2018).

$$V = -\frac{Q}{A\varepsilon_o} + \left(d_o + x(t)\right) + \frac{\sigma x(t)}{\varepsilon_o} \qquad \text{Eq.1}$$

Where:

$d_o = \sum_{i=1}^{n} \frac{d_i}{\varepsilon_{ri}}$ Or the adequate thickness of the materials.

d_i = the individual material thickness

ε_{ri} = relative permittivity of each material

σ = surface charge density

A = surface area of the materials.

Equation 1 suggests that the output potential is directly related to the $\frac{d_i}{\varepsilon_i}$ material properties, aside from the mechanical contributions of *A* and *x(t)*.

2. METHODOLOGY

2.1 Synthesis and preparation of GO

The graphene oxide materials, 1XGO and 3XGO, were synthesized following a modified Hummer's method utilizing a preformed acidic oxidizing medium (C.-H. Chen et al., 2017; Ebajo et al., 2019). The preformed acidic oxidizing medium used for the synthesis of 1XGO was prepared by mixing 23 mL of H_2SO_4 (98%) with P_2O_5 (1 g) followed by addition of $KMnO_4$ (3 g) for 3 min. Graphite flakes (1g, Alfa Aesar, 325 mesh) and $NaNO_3$ (0.5 g) were ground into a uniform mixture and introduced into the preformed acidic oxidizing medium. After 10 minutes, the mixture was heated and vigorously stirred in an oil bath maintained at 35 °C for 1 hour. Portions of DI water (10 mL) were successively added five times to prevent overheating from the exothermic reaction. The resulting mixture was then warmed to 85 °C for 15 min. After cooling to room temperature, H_2O_2 (10 mL, 35%) was slowly added. Filtration of the reaction mixture followed by subsequent washing with 1M HCl and distilled water yields 1XGO as a black powder. 3XGO was prepared using a preformed acidic oxidizing medium composed of 23 mL of H_2SO_4 (98%), P_2O_5 (1 g), and $KMnO_4$ (9 g). The 1XGO and 3XGO samples were placed on individual substrates consisting of a standard microscope slide (75mm x 25mm x 1mm) by blading procedure. Excess GO materials were scraped using the corners of glass slide serving as a blade to produce a uniform flat surface. These glass slides coated with 1XGO and 3XGO served as the lower-based VCS GiTO -TENG assembly. During this study, most of the experimental output was focused on 1XGO.

2.2 Fabrication and electrical characterization of GiTO-TENG.

The lower assembly of the GiTO-TENG - which was made of the 1XGO sample- was constructed by attaching a 3M " magic tape®" at both ends of the glass slides, which serves as spring motion and separator with ends connected to the upper assembly shown in figure 2a. The upper assembly consists of a commercially available ITO film on a PET substrate film (Sigma Aldrich: Pcode#0002220541) attached to a 0.1mm thick PVC book cover by double-sided tape. The separation distance between the lower and upper assembly is approximately 5mm. An AWG 18 insulated copper wire was used as an electrode for Graphene and ITO film. The wire is attached to the surface of the graphene by an aluminum foil tape. In

contrast, the other wire is attached to the ITO surface using similar aluminum foil tape to provide electrical connectivity. The electrical test used a digital oscilloscope (Agilent Technologies DSO-X 2002A) with a passive 100MΩ probe.

2a

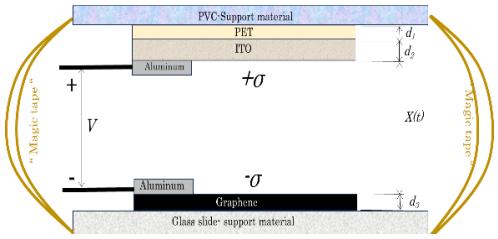

2b

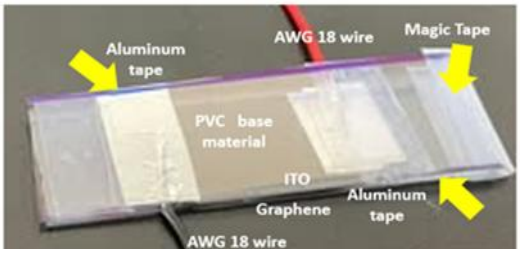

Fig. 2 a) Illustration of GiTO-TENG, showing the layers of materials. b) The actual photo of GiTO-TENG

An estimated downward force of 4N using hand tapping was applied to the device to generate output. To verify the GiTO-TENG durability, a linear actuator was used to press/ release the TENG at approximately 4.34Hz with a total cycle of 109 cycles. All experiments were performed inside a clean laboratory at 21 ± 2°C and a relative humidity of 62 to 67%.

3. RESULTS AND DISCUSSION

Figure 3 shows open circuit output voltage when hand tapping was used as a vertical downward force. The Inset photo of Figure 3 shows the details of one of the pulses, wherein there is peak positive voltage, where the separation distance, *x(t),* is maximum. When the x(t) → 0, the voltage returns to zero to complete the peak. However, due to the spring action of the separator, the upper part moves upward when *x(t)* → *d*, the polarity reverses, and the negative voltage follows immediately.

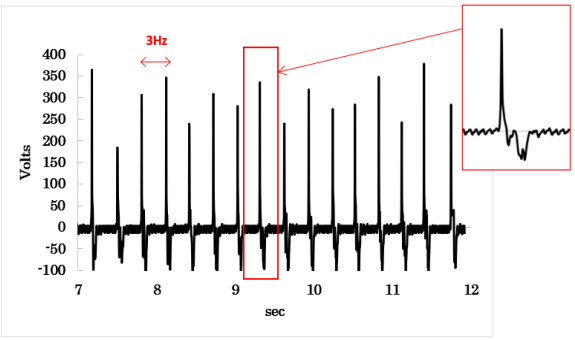

Fig. 3. Open circuit voltage during hand tapping of the GiTO-TENG. A maximum voltage of 505 V_{pp} with a frequency of 3Hz. Inset picture the pulse shape.

To compute the power density, the rms voltage of the GiTO-TENG was computed first using the relation (Benitez, 2019):

$$V_{rms} = \sqrt{\frac{\sum x^2}{n}} \qquad \text{Eq.2}$$

Where: x^2 = is the individual data points collected during measurements.
n = is the number of data points

The power density is computed by $P = {V_{rms}^2}/{A\,R_L}$, where R_L is the load resistance and A is the active area (400mm²) of both graphene and ITO film. Figure 4 shows the power density and the calculated current across the load resistor of the GiTO-TENG. The current at the load is computed by $I = {V_{rms}}/{R_L}$.

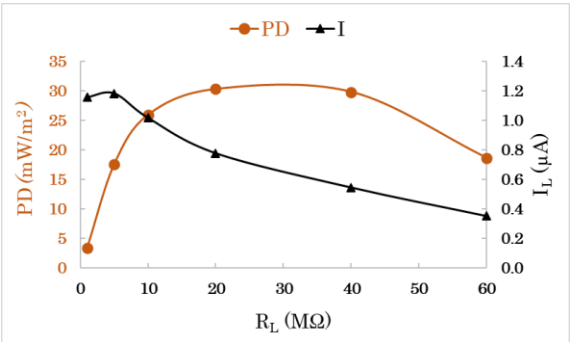

Figure 4. Calculated power density for different load resistors.

The chart shows the power density (PD) was attained at 20MΩ load, with a calculated current of 0.78μA. The PD continues until it slightly decreases at 40MΩ and significantly attenuates at 60MΩ. This data infers that efficient TENG operations require a high resistive load, usually between 5MΩ and 40MΩ for efficient operations (H. Chen et al., 2018). Figure 5 shows the calculated rms voltage (V_{rms}) and power across (P_L) the load resistors R_L.

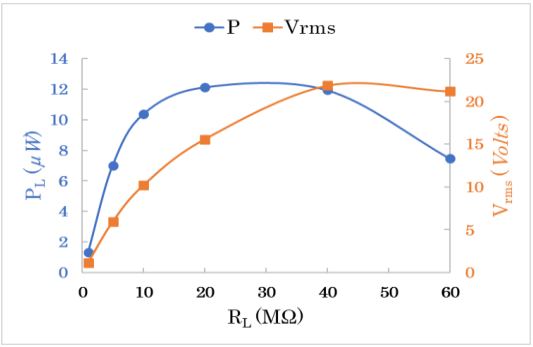

Fig. 5. Power across and rms voltage across different load resistors.

The graphs show a cross-over of the V_{rms} and the P_L, which indicates the optimum resistive load for efficient operations. To test the long-term operations of the device, figure 6 shows the stability of GiTO-TENG using a linear actuator at 4.3 Hz or

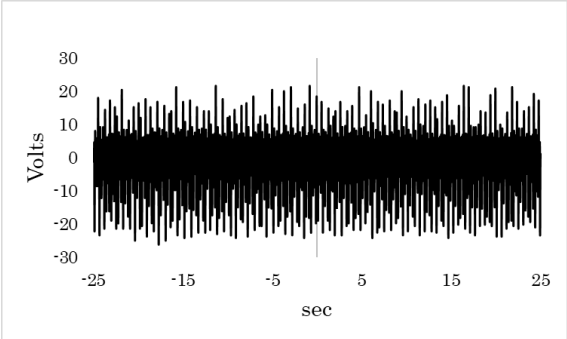

Fig. 6, GiTO-TENG stability during a 109-cycle test using a linear actuator. The frequency was approximately 4.3 Hz.

109 cycles. The results show that there is no indication of degradation during the test. The voltage output during this test is lower than manual tapping since the force applied is much lower to avoid breaking the glass substrate of the GiTO-TENG. The GiTO-TENG could light up 19 LEDS, as shown in the photo of Figure 7.

Fig. 8 shows the 19 LEDS in series light up during hand tapping.

Lastly, 3XGO (more oxidized material) was compared with the 1XGO GiTO-TENG. Figure 8 compares a single hand tapped by applying a tapping force 5N,

which was recorded at 5ms/div from a digital oscilloscope.

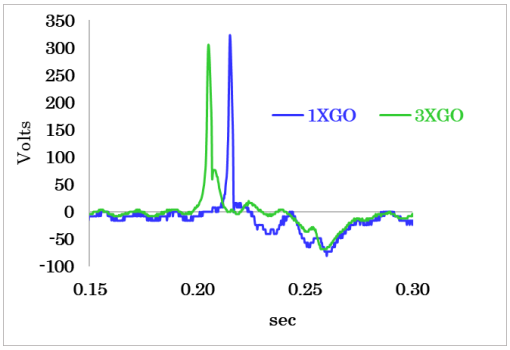

Fig. 8. Comparison of 1XGO and 3XGO. The 1XGO has a slightly higher output due to better film quality.

The 1XGO is 12% higher in V_{pp} compared with 3XGO. Factors such as amount of oxygen and extent of π-conjugation in the graphene oxide surface may contribute to the difference in the observed performance of the samples. It is also worth noting that the 1XGO sample forms a better film quality compared with 3XGO which may affect their performance. Further studies are being conducted by our group to explore the difference in the performance of the two graphene oxide materials. On the other hand, the output voltage of this GiTO-TENG is significantly higher than the previously reported. Table 1 compares the similarly fabricated graphene-based TENG from published articles:

Table 1: Comparison of Graphene-based TENG

TENG	A (mm^2)	V_{pp} (Volts)	Published work
1XGO/ ITO/PET-Al Electrode	400	348	This work
PDMS//SEG/ Polyimide-Al electrode	625	233	(Domingos et al., 2021)
Graphene/EVA/PET-PDMS/ITO-Cu electrode	896	650	(Shankaregowda et al., 2016)
GO/Al/PTFE-Cu electrode	1600	1100	(Guo et al., 2017)

4. CONCLUSIONS

We can fabricate a compact 20 x 20mm 1XGO-based TENG (GiTO-TENG) and be able to generate a maximum peak-to-peak voltage of 348Volts and a current of 0.78μA at a load resistor of 20MΩ. The device also generated a rms voltage of 21.18 Volts and 12 μW across a load of 40MΩ, which is enough to light up 19 LEDs. The output of this compact GiTO-TENG is comparatively better than that of previously reported TENGs.

The TENG devices fabricated using 1XGO and 3XGO resulted in a comparable output voltage, with 1XGO delivering a slightly higher output. Further studies are needed to elucidate the factors that resulted in their performance difference.

5. ACKNOWLEDGMENTS

The authors would like to acknowledge Dr. Carla Manzano of the Department of Physics -DLSU for providing the generous amount of ITO films used in this project. To Dr. Alex Co Abad, Engr. Dino Ligutan and Mr. William De Guzman, who are from the department of ECE -DLSU, for allowing the corresponding author to use the Digital Oscilloscope.

6. REFERENCES

Benitez, V. H. (2019). Pattern Classification and Its Applications to Control of Biomechatronic Systems. In *Artificial Neural Networks for Engineering Applications* (pp. 139–154). Elsevier. https://doi.org/10.1016/B978-0-12-818247-5.00020-4

Chakraborthy, A., Nuthalapati, S., Nag, A., Altinsoy, M. E., & He, S. (2024). Graphene-based triboelectric

nanogenerators for energy-harvesting applications. In *Sensors and Actuators A: Physical* (Vol. 380). Elsevier B.V. https://doi.org/10.1016/j.sna.2024.116046

Chen, C.-H., Hu, S., Shih, J.-F., Yang, C.-Y., Luo, Y.-W., Jhang, R.-H., Chiang, C.-M., & Hung, Y.-J. (2017). Effective Synthesis of Highly Oxidized Graphene Oxide That Enables Wafer-scale Nanopatterning: Preformed Acidic Oxidizing Medium Approach. *Scientific Reports*, *7*(1), 3908. https://doi.org/10.1038/s41598-017-04139-0

Chen, H., Xu, Y., Zhang, J., Wu, W., & Song, G. (2018). Theoretical System of Contact-Mode Triboelectric Nanogenerators for High Energy Conversion Efficiency. *Nanoscale Research Letters*, *13*. https://doi.org/10.1186/s11671-018-2764-2

Domingos, I., Neves, A. I. S., Craciun, M. F., & Alves, H. (2021). Graphene Based Triboelectric Nanogenerators Using Water Based Solution Process. *Frontiers in Physics*, *9*. https://doi.org/10.3389/fphy.2021.742563

Ebajo, V. D., Santos, C. R. L., Alea, G. V., Lin, Y. A., & Chen, C.-H. (2019). Regenerable Acidity of Graphene Oxide in Promoting Multicomponent Organic Synthesis. *Scientific Reports*, *9*(1), 15579. https://doi.org/10.1038/s41598-019-51833-2

Fang, Y., Ao, C. K., Jiang, Y., Sun, Y., Chen, L., & Soh, S. (2024). Static charge is an ionic molecular fragment. *Nature Communications*, *15*(1). https://doi.org/10.1038/s41467-024-46200-3

Guo, H., Li, T., Cao, X., Xiong, J., Jie, Y., Willander, M., Cao, X., Wang, N., & Wang, Z. L. (2017). Self-Sterilized Flexible Single-Electrode Triboelectric Nanogenerator for Energy Harvesting and Dynamic Force Sensing. *ACS Nano*, *11*(1), 856–864. https://doi.org/10.1021/acsnano.6b07389

Lin, Z., Long, W., Chen, L. J., Niu, S., & Zi, Y. (2016). *Green Energy and Technology Triboelectric Nanogenerators*. Springer International Publishing, Switzerland. https://doi.org/10.1007/978-319-40039-6

Macá, D., Domingos, I., Carvalho, N., Pinho, P., & Alves, H. (2022). iScience Harvesting circuits for triboelectric nanogenerators for wearable applications. *ISCIENCE*, *25*, 103977. https://doi.org/10.1016/j.isci

Navaneeth, M., Supraja, P., Babu, A., Uday Kumar, K., Prakash, K., & Rakesh Kumar, R. (2023). A triboelectric nanogenerator based on commercial ITO-PET sheets for mechanical energy harvesting and self-powered indicator display applications. *Materials Letters*, *336*. https://doi.org/10.1016/j.matlet.2023.133866

Olson, K. P., & Marks, L. D. (2024). What Puts the "Tribo" in Triboelectricity? *Nano Letters*, *24*(39), 12299–12306. https://doi.org/10.1021/acs.nanolett.4c03656

Seol, M., Kim, S., Cho, Y., Byun, K. E., Kim, H., Kim, J., Kim, S. K., Kim, S. W., Shin, H. J., & Park, S. (2018). Triboelectric Series of 2D Layered Materials. *Advanced Materials*, *30*(39). https://doi.org/10.1002/adma.201801210

Shankaregowda, S. A., Nanjegowda, C. B., Cheng, X. L., Shi, M. Y., Liu, Z. F., & Zhang, H. X. (2016). A flexible and transparent graphene-based triboelectric

nanogenerator. *IEEE Transactions on Nanotechnology*, *15*(3), 435–441. https://doi.org/10.1109/TNANO.2016.2540958

Sobarzo Ponce, J. C. W. S. (2023). A triboelectric series of identical materials. *APS March Meeting April 2023*, 1–1. Https://uiadsabs.harvard.edu/abs/2023..APSMARBO7008S/abstract

Wang, Z. L. (2013). Triboelectric nanogenerators as new energy technology for self-powered systems and as active mechanical and chemical sensors. In *ACS Nano* (Vol. 7, Issue 11, pp. 9533–9557). https://doi.org/10.1021/nn404614z

Wang, Z. L., & Wang, A. C. (2019). On the origin of contact-electrification. In *Materials Today* (Vol. 30, pp. 34–51). Elsevier B.V. https://doi.org/10.1016/j.mattod.2019.05.016

Zhang, R., & Olin, H. (2020). Material choices for triboelectric nanogenerators: A critical review. In *EcoMat* (Vol. 2, Issue 4). John Wiley and Sons Inc. https://doi.org/10.1002/eom2.12062